Supporting Information

Sevrioukova and Poulos 10.1073/pnas.1010693107

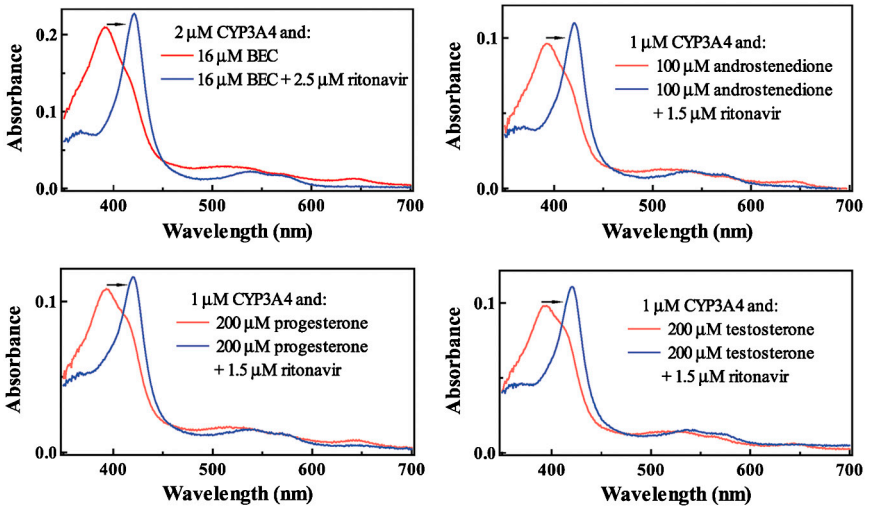

Fig. S1. Ritonavir replaces type I substrates bound to CYP3A4. Addition of a slight excess of ritonavir to the bromoergocryptine (BEC)-, progesterone-, androstenedione-, or testosterone-bound CYP3A4 leads to an immediate high-to-low spin shift.

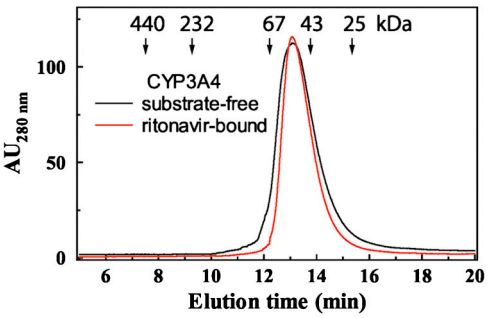

Fig. S2. Gel filtration elution profile of ligand-free and ritonavir-bound CYP3A4. The protein was eluted from the Superdex 200 FPLC column in 50 mM phosphate (pH. 7.5) and 100 mM NaCl. Arrows indicate elution time for molecular standards: 1- ferritin, 440 kDa; 2 - catalase, 232 kDa; 3 - albumin, 67 kDa; 4 - ovalbumin, 43 kDa; and 5 - chymotrypsinogen A, 25 kDa.

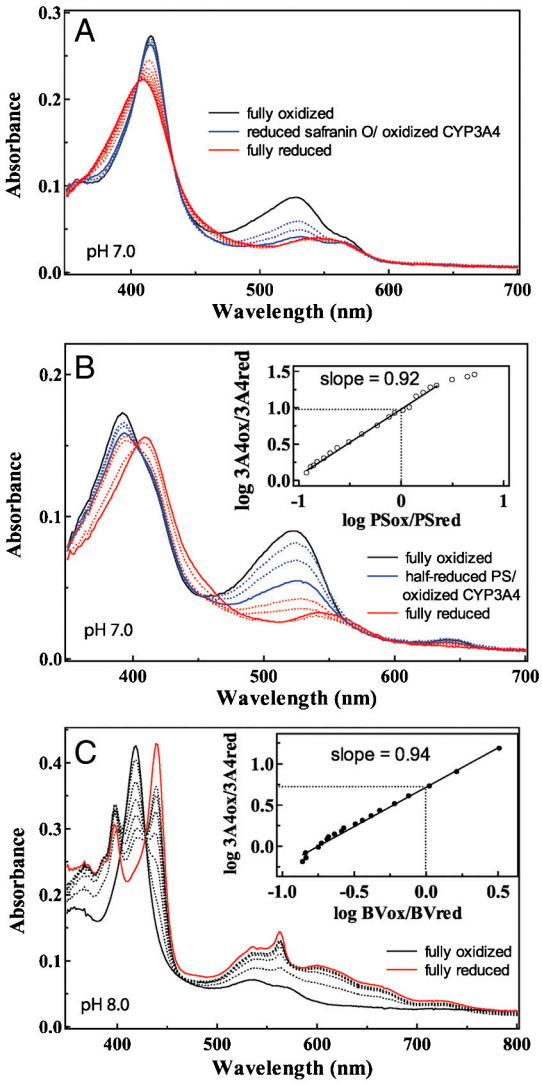

Fig. S3. Spectroscopic determination of the CYP3A4Δ3-24 redox potentials. Anaerobic mixtures contained xanthine-saturated 100 mM phosphate (various pH), 2–4 μM CYP3A4 and 1–2 μM redox dyes: safranin O (−280 mV), phenosafranin (PS, −247 mV) or benzyl viologen (BV, −359 mV). Reactions were initiated by addition of catalytic amounts of xanthine oxidase (Sigma). Sodium dithionite was added at the end to fully reduce CYP3A4 and the redox mediator. Reduction of ligand-free CYP3A4 starts after safranin O gets fully reduced (*A*), indicating that the P450 redox potential is at least 50 mV lower ($\cong -330$ mV). The $E_{o,7}$ values for androstenedione- and ritonavir-bound CYP3A4 were estimated from the absorbance changes at 410/515 and 442/650 nm (*B* and *C*, respectively) and were equal to -277 ± 7 and -350 ± 5 mV, respectively.

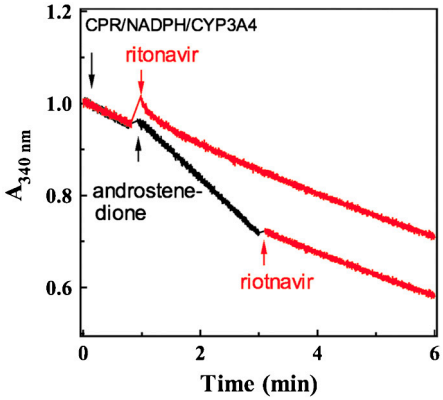

Fig. S4. Consumption of NADPH in the CYP3A4-CPR reconstituted system. Reaction mixtures contained 1.7 μM CYP3A4 and 1.7 μM CPR in 50 mM phosphate buffer, pH 7.5. The base rate was measured in the presence of 125 μM NADPH at 340 nm and 30 °C, after which either ritonavir or androstenedione were added (30 and 200 μM final concentration, respectively). The NADPH oxidation rate does not change in the presence of ritonavir but is increased upon addition of a type I substrate androstenedione. This indicates that androstenedione but not ritonavir is metabolized by CYP3A4.

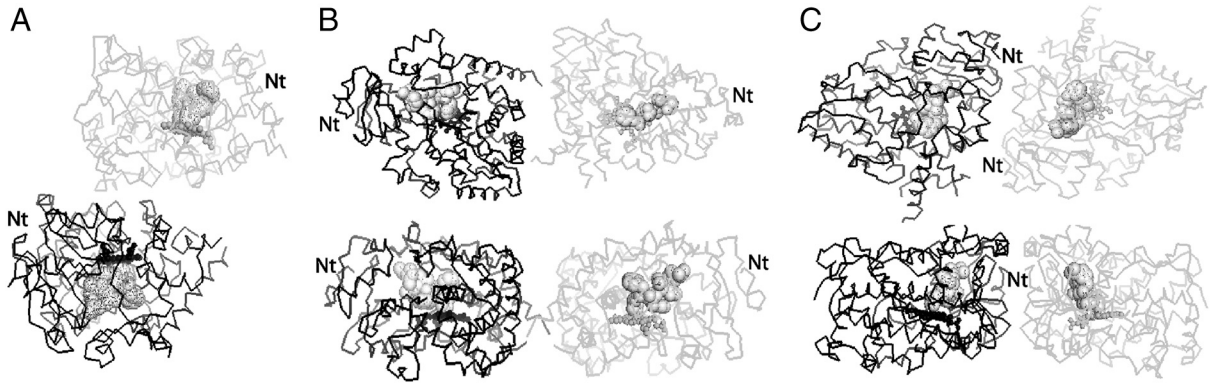

Fig. S5. Three types of monomer-monomer contacts in the crystals of ritonavir-bound CYP3A4. The heme and ritonavir are in stick and CPK representation, respectively.

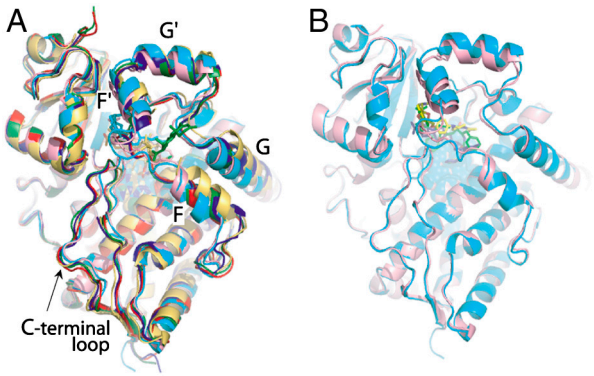

Fig. S6. Comparison of the CYP3A4 structures. (*A*), Structural overlay of substrate-free CYP3A4 (1TQN, blue) and its complexes with ritonavir (pink), metyrapone (1WOG, red), progesterone (1WOF, green), erythromycin (2JOD, yellow), and ketoconazole (2VOM, cyan). Only structural elements that undergo notable conformational changes upon substrate/inhibitor binding are labeled. (*B*), The CYP3A4-ritonavir complex (pink) is most similar to the ketoconazole-bound CYP3A4 structure (cyan). The CYP3A4 ligands and the heme are in stick and CPK representation, respectively.

Table S1. Data collection and refinement statistics

Data statistics	
Space group	C2
Unit cell parameters	$a = 162$ Å, $b = 95$ Å, $c = 93$ Å, $\beta = 124°$
Resolution range	77.4–2.0 (2.05–2.0) *
Total reflections	285, 541
Unique reflections	76, 811
Redundancy	3.7 (3.8)
Completeness	98.0 (97.4)
Average $I/\sigma I$	10.8 (4.6)
R_{merge}	0.064 (0.35)
Refinement statistics	
Molecules per asymmetric unit	2
R/R_{free} †	23.2/26.2
Average B-factor, Å^2	44.3
rms deviations	
Bond lengths Å	0.016
Bond angles °	1.4

*Values in brackets are for the highest resolution shell.
†R_{free} was calculated from a subset of 5% of the data that were excluded during refinement.